

## **Improving megasonic exposure uniformity for EUV mask substrate cleaning**

Matthew House<sup>1</sup>, Abbas Rastegar<sup>1</sup>, Don Dussault\*<sup>2</sup>, Eric Liebscher<sup>2</sup>

<sup>1</sup>SEMATECH, 257 Albany, NY 12303, USA,

<sup>2</sup>ProSys, Inc. 1745 Dell Avenue, Campbell CA, USA

To achieve surface roughness and flatness requirements, EUV mask substrates should undergo chemical mechanical polishing (CMP). These processes can generate both pit and embedded particles on the surface of low thermal expansion material (LTEM) masks. Megasonic-induced pits are one of the critical defectivity modes for EUV mask blank substrates. Pit defects are generated by cavitation collapse near the surface. This work compares a conventional megasonic nozzle system and a proximity-type radially uniform megasonic system with respect to pit creation. In typical cleaning processes used to remove particles on EUV substrates, the megasonic nozzle generates about 3 times more pits than the radially uniform megasonic system. These pits are located at the center of the plate. Distribution of pits generated by the radially uniform proximity system is uniform throughout the plate as megasonic exposure is uniform across the plate.

### **Megasonic cleaning of EUV mask substrates**

Defectivity and surface quality requirements for EUV masks present the most challenges for existing surface cleaning technologies. For manufacturing devices for 16 nm half-pitch DRAMS, all defects larger than 12 nm should be removed from the surface of the low thermal expansion material (LTEM) substrate without changing its surface roughness and flatness. Defects on top of the substrate are pits (voids) and particles. Pits are usually created when the substrate is polished or cleaned; particles are added during chemical mechanical polishing (CMP) or subsequent cleaning and handling.

Cleaning-induced pits are the main cause of defectivity on EUV mask blanks and substrates (1). However, the zero defect requirements for substrates demand that all particles including those embedded in the substrates be removed. Therefore, megasonic cleaning is essential to remove these hard particles; conversely, megasonic cleaning can also create pits on the surface.

The cleaning challenge then is to balance megasonic processes in such a way that maximum particle removal efficiency is obtained without damaging the surface (i.e., creating pits). This article compares the particle removal ability of the megasonic nozzle system currently used at SEMATECH with an alternative wide area proximity megasonic system.

## Nozzle megasonic system

SEMATECH uses the Hamatech (Suss MicroTec) MaskTrack cleaning tool, which commonly incorporates a Sonosys nozzle megasonic system. Megasonic frequencies from 1 to 4 MHz are currently available for Sonosys megasonic systems. The megasonic nozzle can be configured for a single frequency megasonic beam or two overlapping beams with different frequencies. A high megasonic energy can usually be achieved using these nozzles. Assuming ideal impedance matching, the maximum power density with a 1 MHz Sonosys nozzle near the transducer is calculated to be  $\sim 218 \text{ W/cm}^2$  (2). However, the actual power near the transducer is expected to be on the order of 10s of  $\text{W/cm}^2$  due different energy loss mechanisms. Furthermore, transducers in this configuration operate at about 40 to 50 mm from the surface of the mask; therefore, the actual power at the surface is less due to transmission losses.

Figure 1 shows the megasonic nozzle geometry. The impact area of the megasonic beam is a 4 mm circle when the beam is perpendicular to the surface, which will change to an elliptical cross-section when the beam is tilted. To cover the whole mask surface, the nozzle is mounted on an arm with a radius of  $R$  that swings over the surface with an angular velocity of  $\Omega$ . A plate is mounted on a chuck that rotates at an angular velocity of  $\omega$ . The area scanned by megasonic nozzle is a circle with the same diameter as the mask width (152 mm) as shown in Figure 1. Note that the four corners of the mask are not directly exposed to the megasonic beam but will indirectly receive some level of the acoustic field by coupling through the substrate and liquid layer.

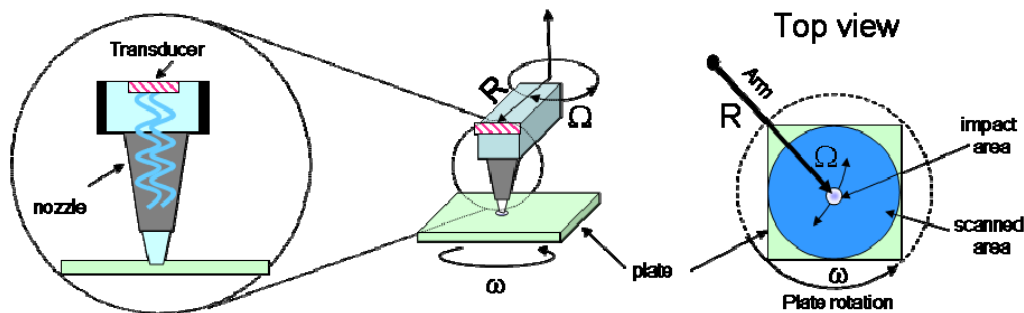


Figure 1 Schematic of a megasonic nozzle (left) with a piezoelectric transducer mounted on top and covered with liquid, which flows through a conical nozzle to the surface. Schematic of the nozzle arm (middle) and top view of the nozzle and plate (right).

This megasonic system is able to remove partially embedded particles, giving impressive results in early substrate cleaning development at SEMATECH (3). By improving SEMATECH's defect inspection capability, early evidence of megasonic-induced pits on quartz substrates was reported (4). The location of the pits coincided with the area scanned by the 1 MHz nozzle. Figure 2 shows defect maps of a quartz and a Ru-capped blank inspected at SEMATECH using the Lasertec M7360, which has a sensitivity of 30 nm sphere equivalent volume diameter (SEVD) on quartz and the Lasertec M1350, which has a sensitivity of 62 nm ( $\text{SiO}_2$  equivalent size) on Ru-capped blanks. Circles show the area scanned by the megasonic nozzle as described in Figure 1.

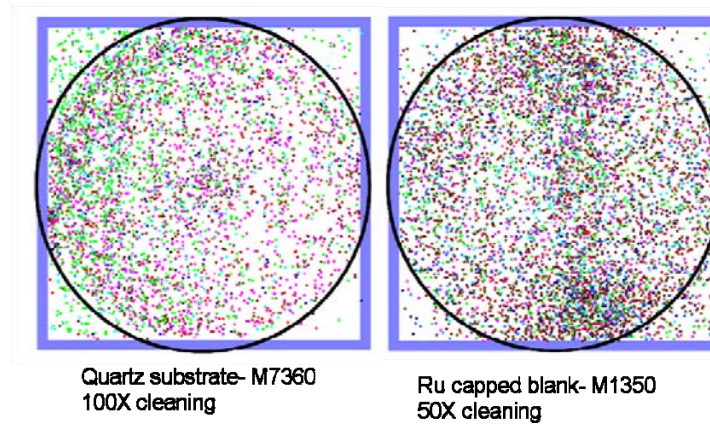


Figure 2 Defect map of a quartz substrate inspected by the Lasertec M7360 after being cleaned 100 times (left) and similar data for a Ru-capped MoSi multilayer blank cleaned 50 times and inspected by SEMATECH's Lasertec M1350. Circles show the area scanned by the megasonic nozzle.

Atomic force microscopy (AFM) analyses show that the majority of these defects are pits. A correlation of pit location with the area scanned by the megasonic nozzle indicates that the megasonic cleaning is responsible for the pits. Note that pit dimensions will change depending on the surface material properties and megasonic power.

As shown in Figure 1, in Hamatech tools the area scanned by the megasonic nozzle is circular, but the megasonic exposure time is not uniform throughout the scanned area. The center of plate is exposed to the megasonic waves for longer than the edge of the plate. In principle, non-uniformity can be improved by controlling the arm and chuck rotation speed ( $\Omega$  and  $\omega$ ) as a function of the location of the megasonic beam on the plate. An alternative solution is to radially change the exposure area, which implies that the exposure area will increase closer toward the edge.

### **MegPie megasonic system**

The MegPie (5) is a wedge-shaped, large area transducer that operates in the direct proximity of the substrate surface. Its shape assures radial uniformity of the acoustic energy delivered to rotating substrate. A single crystal sapphire is used as the resonator material. It is mechanically stable, resistant to and compatible with a wide range of process chemistries, and is an excellent conductor of sound. Applications in wafer cleaning have shown that this transducer generates no sapphire particles (6).

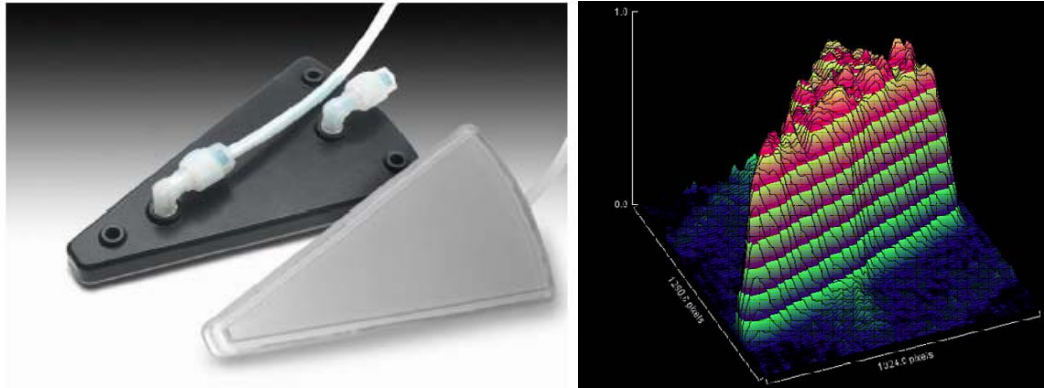


Figure 3. Sonoluminescence imaging indicating cavitation density and uniformity in the acoustic field of a 300 mm MegPie transducer, with energy of  $2.9 \text{ W/cm}^2$  at 925 kHz. Each color cycle = 10%.

## Experiments

To evaluate the MegPie transducer, it was positioned manually on top of the mask inside a cleaning chamber of a modified Hamatech MaskTrack tool, as shown in Figure 4.

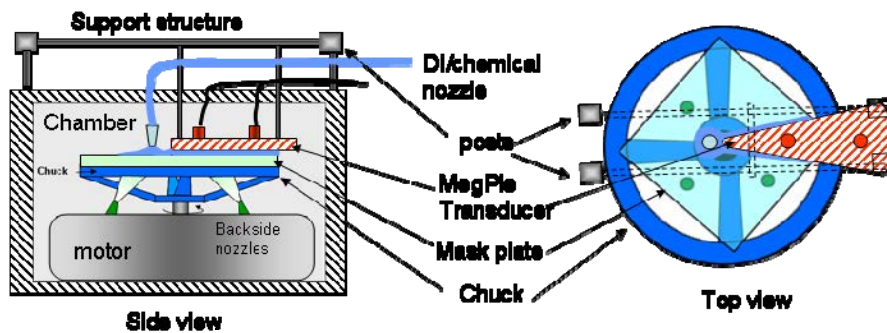


Figure 3 MegPie setup inside the cleaning chamber.

In the first set of experiments, optimized process parameters were determined using megasonic power reflected from the surface by the transducer. These parameters included the distance between the transducer and the plate, fluid flow, and plate rotation speed. Note that unlike the conventional nozzle configuration, megasonic flow management for the MegPie transducer is very critical. All the above parameters should be optimized such that a uniform layer of liquid forms under the transducer area and remains continuous during mask rotation.

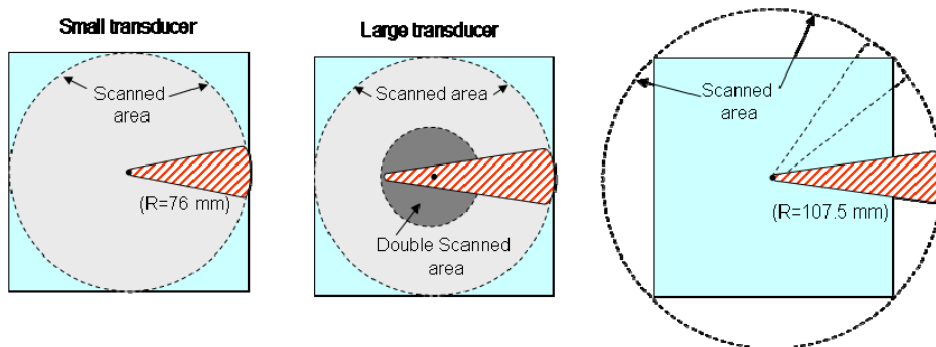


Figure 4 Different configurations of the MegPie with respect to the mask substrates. Note that its diameter is different in different configurations.

With the MegPie transducer, mask form factor introduces some complications. The mask is square and does not have continuous rotational symmetry. Figure 4 shows three possible ways to position the MegPie transducer. In the first case, if the transducer's diameter is designed such that the active area is 76 mm long (i.e., half of the mask side), then the scanned area is a circle confined to the inner surface of the mask. The scanned area is similar to the megasonic nozzle's area in Figure 1; however, due to the MegPie's shape, the whole scanned area is exposed uniformly. In the middle configuration, when the transducer is larger than 76 mm, part of the center will be exposed twice; therefore, the megasonic exposure will not be uniform. In the third configuration, the length of the transducer is half the diameter of the mask ( $R=107.5$  mm). The entire mask surface, including corners, are exposed to a uniform amount of Megasonic energy. However, the overlapping surface between the mask surface and transducer surface is not constant; it changes depending on the orientation of the plate with respect to the mask. The corners receive maximum coverage while coverage is minimum when the transducer is perpendicular to the side of the mask, as shown in Figure 4. Note that in this case, a portion of the transducer surface is not covered with water during the full mask rotation cycle. This may cause particles to dry on the transducer surface and then transfer to the mask, an issue that should be addressed in future iterations of the MegPie.

In our studies, we used a prototype 150 mm long MegPie transducer designed for 300 mm wafer cleaning. It was positioned as shown in Figure 1. Initially, the transducer was rinsed with deionized (DI) water for 15 hours. Figure 6 shows the Lasertec M1350 defect maps of two plates cleaned with the MegPie under optimized and non-optimized conditions. All defects larger than 43 nm SEVD are shown. The first column shows defect maps before cleaning; middle column, defects after cleaning and last column, defects added by cleaning. When the key parameters—flow rate, transducer gap, and plate rotation speed—are not optimized, a streak of particles can be added to the surface. Added particles are about 5 nm high and 100 nm wide. An example of such a particle is shown in Figure 5. This particle has a faceted surface, which is typical of crystalline material. Attempts to determine its composition using electron-dispersive spectroscopy (EDS) and Auger nanoscopy were not successful as the particle dimensions were too small to obtain reasonable signals. A typical MegPie megasonic-generated pit is also shown, which is similar to those created by nozzle megasonics.

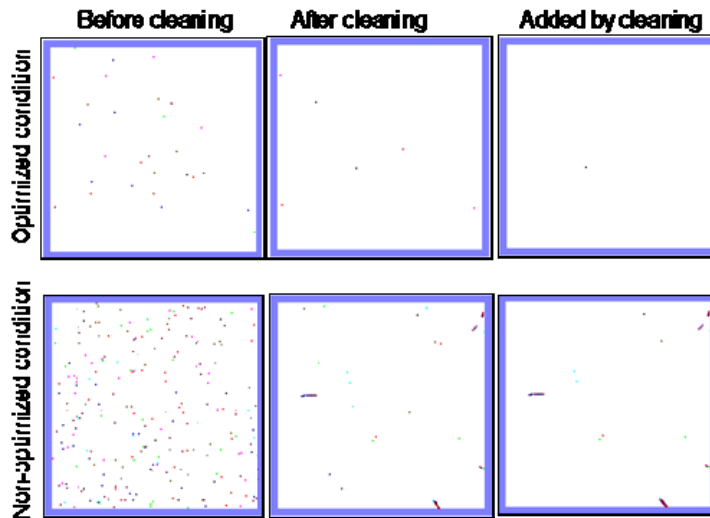


Figure 5 Lasertec M1350 defect maps of two plates. The top row was cleaned under optimized conditions and the bottom row with a non-optimized cleaning process. The first column shows defect maps before cleaning, middle column after cleaning, and last column added by cleaning.

Optimized cleaning starts with a DI water rinse followed by an ammonium hydroxide/hydrogen peroxide/DI water mixture (APM) and final DI water rinse. The megasonic transducer is active during the entire process. On a plate with native defects, the particle removal efficiency (PRE) was 99.4% and cleaning efficiency (CE) was 95% for all defects larger than 50 nm.

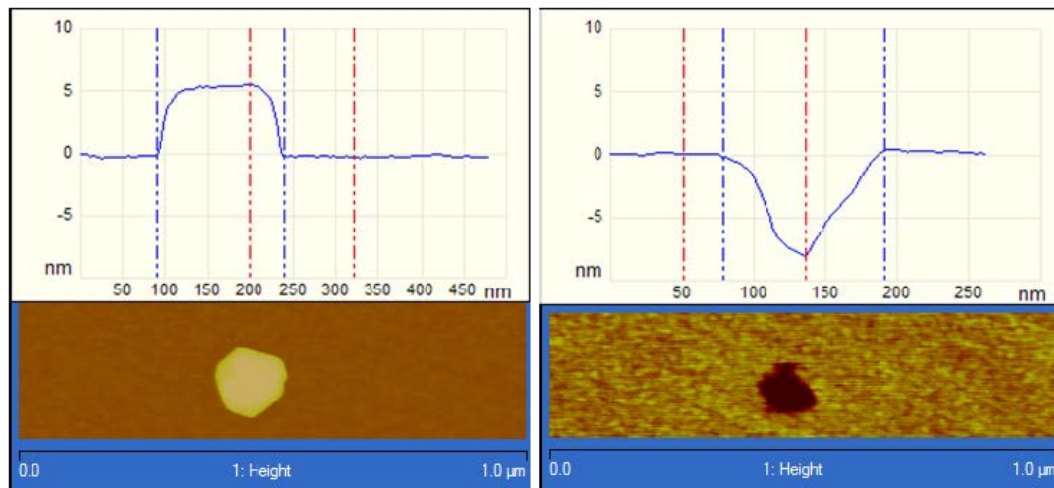


Figure 6 AFM images of particles (left) and pits (right) added during cleaning by the MegPie system.

To study pits left by different megasonic systems, a set of experiments was performed on quartz and LTEM using the nozzle and MegPie systems. Figure 7 shows pits larger than 32 nm SEVD added by both systems on LTEM substrates during multiple cleaning cycles, which indicates that both transducers generate cavitation when using applied acoustic power. However, as expected, pits generated by the megasonic nozzle



are concentrated at the center and those created by the MegPie are distributed throughout the plate. This behavior is due to the non-uniform exposure of the nozzle system as it is currently configured in Hamatech mask cleaning tools. Figure 7 also shows the megasonic nozzle leaves more pits than the MegPie, in keeping with their different exposure times.

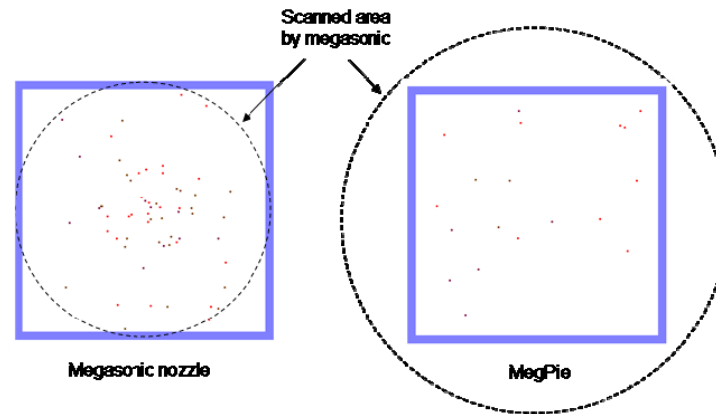


Figure 7 Lasertec M7360 defect maps of two LTEM substrates after 120 min exposure to megasonic nozzle (left) and 90 min exposure to MegPie transducer (right).

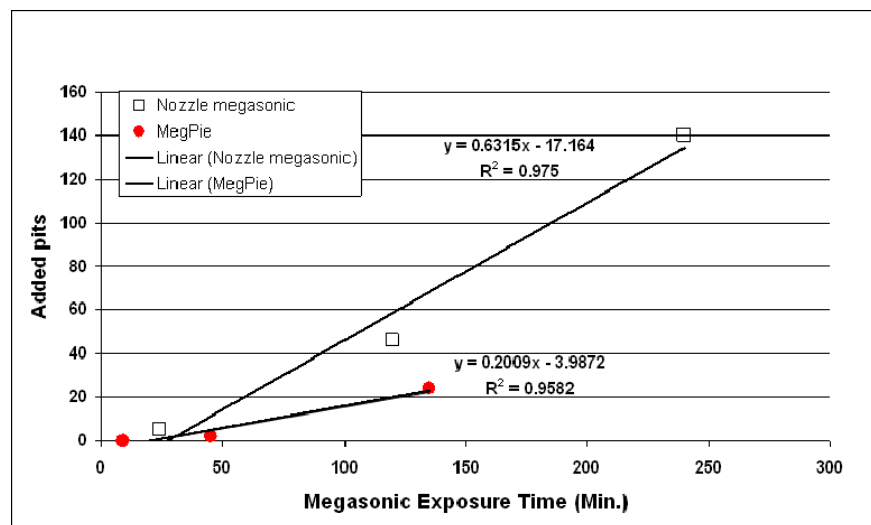


Figure 8 shows the number of the pits created on quartz substrates as a function of the megasonic exposure time for both transducers.

The number of megasonic-induced pits vs. megasonic exposure time is plotted in Figure 8. As can be seen, the rate of pit generation with a megasonic nozzle is almost 3 times that of the MegPie. Note that these two transducers operate under different acoustic power at the mask surface. As was shown in Figure 3, the acoustic power distribution is uniform with the MegPie, but it is not uniform with the nozzle megasonic because of acoustic interference effects in the conical nozzles. In some locations, the acoustic power is above the transient cavitation threshold, which results in violent cavitation collapse that may cause a higher pit density.

### Acknowledgments

The authors would like to thank their colleagues in SEMATECH's EUV Mask Blank Development Center in Albany for their continuous support in cleaning and Aron Cepler for AFM images of the particle and pits.

### References

1. A. Rastegar, A. J. Kadaksham, B. Lee, M. House, J. Sohn, D. Ashworth, M. Kishimoto and J. Choi, *EUVL Symposium*, Kobe, Japan (2010)
2. A. Rastegar, S. Eichenlaub, A. John, B. Lee, M. House, S. Huh, B. Cha, H. Yun, I. Mochi, and K. Goldberg *Proc. of SPIE* **7636**, 76360N (2010)
3. A. Rastegar, Y. Ikuta, S. Eichenlaub, K. Goncher, H. Popp, and P. Marmillion, *EUVL Symposium*, San Diego, USA (2005)
4. A. Rastegar, S. Eichenlaub, V. Kapila, A. John Kadaksham, and P. Marmillion, *Proc. of SPIE* **6921**, 6921 (2008)
5. Beck et al., Radial Power Megasonic Transducer US patent 6,791,242 (2004).
6. D.Dussault, F.Fournel, V.Dragoi, High efficiency single wafer cleaning for wafer bonding-based 3d integration applications, p. 190 *UCPSS Abstracts*, (2010)
7. Beck et al., Chemically Inert Megasonic Transducer System, US Patent 6,222,305 (2001).